# Optoacoustic endoscopy with optical and acoustic resolution

Hailong He [a,b], , Georg Wissmeyer [a,b] Saak V. Ovsepian [a,b], Andreas Buehler [a,b], and Vasilis Ntziachristos [a,b*]

[a] *Institute for Biological and Medical Imaging, Helmholtz Zentrum München, Ingoldstädter Landstraße 1, 85764 Neuherberg, Germany*
[b] *Chair for Biological Imaging, Technische Universität München, Ismaninger Str. 22, 81675 München, Germany*

## ABSTRACT

A hybrid optical and acoustic resolution optoacoustic endoscopy is proposed. Laser light is transmitted to tissue by two types of illumination for optical and acoustic resolution imaging respectively. An unfocused ultrasound detector is used for recording optoacoustic signals. The endoscopy probe attains 3.6 mm diameter and is fully encapsulated into a catheter system. We examine the performance of the hybrid endoscope with phantoms and tissue sample, which shows that the hybrid endoscopy can obtain optical resolution in superficial microscopic imaging and ultrasonic tomography reconstruction resolution when imaging at greater depths.

**Keywords:** Optoacoustic endoscopy, optoacoustic imaging, optical resolution, acoustic resolution

## 1. INTRODUCTION

High-resolution optical imaging techniques (e.g., white-light endoscopy, fluorescence microscopy, multi-photon microscopy or confocal microscopy) are commonly employed for endoscopic applications [1, 2]. White light endoscopy (WLE) allows the collection of color video of the entire gastro-intestinal track and can inspect for obstructions and overt stress and damage of the tissue, however it is only capable of visualizing the lumen surface. Confocal laser endomicroscopy (CLE) on the other hand enables subsurface imaging in vivo, which could lead to earlier detection of latent gastrointestinal pathologies or prodromal cancers compared to WLE[2]. Due to intrinsic limitations of pure optical imaging, both modalities have limited imaging penetration depth and interrogate superficial layers of the lumen (<1mm2 at a time), which prevents their application to surveillance endoscopy. In addition, accurate disease readings with fluorescence probes typically require systemic or local administration of reporter agents with high specificity [2].

Label-free optoacoustic imaging allows high-resolution optical interrogation much deeper than intra-vital microscopy[3]. Moreover, detection of histopathological and molecular information can be enhanced by the application of multispectral optoacoustic tomography (MSOT), which can identify different tissue chromophores and exogenous photo-absorbing agents based on changes in their absorption spectra using spectral unmixing techniques[3, 4]. Indeed, MSOT has been shown to reveal several anatomical, pathophysiological (tissue hypoxia, ischemia) or molecular features (expression of receptors and proteases) in vivo [3-5].

Optoacoustic endoscopes, that combine ultrasonic diffraction limited resolution using focused ultrasound detectors, have been proven to achieve from hundreds to tens of micro-meters lateral resolution with an imaging depth up to several millimeters[6, 7]. Improved resolution but limited penetration depth can be achieved by optical-resolution optoacoustic endoscopy using a focused laser beam, in analogy to intra-vital optical microscopy [8-11]. The development of hybrid systems utilizing optical- and ultrasound-resolution optoacoustic systems has been proposed for enhancing the imaging scalability. Herein, we propose a principle of optical resolution (OR) and acoustic resolution (AR) optoacoustic (OR/AR) endoscope to improve the resolution and penetration ability of the hybrid system.

Photons Plus Ultrasound: Imaging and Sensing 2017, edited by Alexander A. Oraevsky, Lihong V. Wang, Proc. of SPIE Vol. 10064, 100641C · © 2017 SPIE · CCC code: 1605-7422/17/$18 · doi: 10.1117/12.2252313

## 2. MATERIALS AND METHOD

### 2.1 Endoscopic imaging configuration

Fig.1 (a) presents the schematic overview of the OR/AR-endoscope. A custom-designed unfocused ultrasound transducer (Imasonic, France) with a center frequency of 20 MHz is used for the detection of ultrasound signals. The diameter of the transducer is 2 mm and the sensing area has a rectangular shape with a length of 0.25 mm and a width of 1.6 mm, yielding an acceptance angle of 80 degrees as derived experimentally from point-source measurements. A GRIN-lens fiber (GT-MMFP-10 μm, GRINTECH, Germany) is secured beneath the transducer for OR illumination. This fiber has a core diameter of 10 μm, a numerical aperture of 0.1, and consisting of a gradient index lens, a coreless spacer and a prism. To align the illumination focus, the GRIN-lens is placed with a tilt angle of 5 degrees in relation to the transducer. Such arrangement prevents the fiber tip from blocking the transmission path of optoacoustic signals. Using a beam profiler (SP620U, OPHIR Beam Gauge, US), we measured the beam diameter based on the full width at half-maximum (FWHM) value, which at the focus region estimates to be ~8.7 μm [Fig. 1(b)]. For implementing AR imaging, a multi-mode fiber (400 μm diameter) with a broad side-view illumination has been aligned with the transducer at a tilt angle of 30 degrees. With such an arrangement, the overlapping areas between the laser beam and the acoustic axis begin at about 1 mm distance from the transducer sensing surface, and extend over a large depth. Illumination is provided by a 532 nm laser, with a pulse repetition rate of 2 kHz and energy of 1 mJ/pulse and pulse width of 0.9 ns (Wedge HB532, BrightSolutions SRL, Pavia, Italy). The beam is attenuated, collimated and guided through a pinhole (Thorlabs) to ensure spatial filtering. It is then passed into a telescopic lens array (Thorlabs) to adjust the beam diameter to match the back aperture of a low NA microscope objective (L-4X, Newport) which is mounted on a manual fiber coupler (F-91TS, Newport). Finally, the beam is tightly focused and coupled into the OR and AR fibers respectively. The light fluence at the surface of the sample is measured about 6 mJ/cm2 for OR imaging and about 10 mJ/cm2 for AR imaging. The recorded optoacoustic signals are amplified by a low noise amplifier (63 dB, AU-1291, Miteq Inc., Hauppauge, New York, USA) and sampled by a high-speed digitizer, operating at 1 GS⁄s (NI PCI-5124, USA; 12 bit resolution; max sampling rate 4 GS⁄s).

The endoscope probe is encapsulated in a medical-grade (polyethylene terephthalate) tube with an outer diameter of 3.6 mm, which can readily pass through 3.8 mm working channels of commercial optical endoscopes. Fig.1(c) shows the enlarged photograph of the probe. To obtain volumetric images, fast linear and rotational stages (Oriental Motor, Japan) were employed. The probe was first scanned linearly along the direction of the lumen and then rotated to get adjacent cross-sectional images. This scanning mode is suitable only for limited-view imaging of the lumen volume, i.e. an imaging mode that is appropriate for operation under optical endoscope guidance, whereby the hybrid optoacoustic endoscope is operated through the working channel of an optical endscope. However, 360-degree rotation could be also contemplated for endoscopes designed to operate in stand-alone mode, i.e. without white-light endoscopy guidance. In the current implementation, OR and AR scans were performed by sequentially coupling the light into the corresponding fiber. The linear and rotational scanning step sizes were 0.01 mm and 0.01 degrees for OR imaging, and 0.08 mm and 0.1 degrees for the AR imaging. Hilbert transform was performed to process the OR data; the filtered back-projection method was used to reconstruct the AR data as described previously [12].

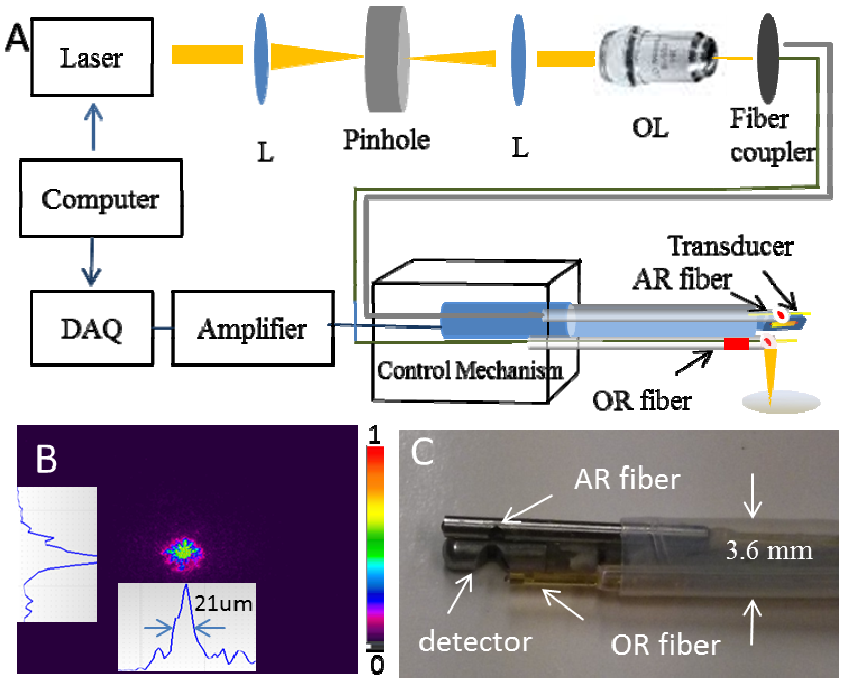


Figure 1 (a) Schematic illustration of the imaging setup with alignment of various modules; Abbreviations: L, Lens; OL, objective lens. (b) Laser beam intensity profile at the focal distance. (c) Photograph of the distal end of the hybrid endoscopy probe.

### 2.2 Phantom and tissue measurements

To characterize the resolution of the system, we measured a phantom with several sutures (10 µm diameter) embedded in scattering agar (6% intra-lipid) at different depths (0.3 mm to 4 mm). The suture positions are illustrated in Fig. 2 (a). In order to quantify the OR resolution, point-spread-functions (PSFs) were measured by imaging the first suture at different distances from the OR fiber. In order to assess the imaging performance of the system on biological specimens, a fresh mouse ear ex vivo was imaged. A luminal structure was casted by rolling the mouse ear inside of a plastic tube. A photograph of the ear imaged prior to rolling was shown in Fig. 3 (a).

## 3. RESULTS

Fig.2 shows the results of characterization phantom experiments. Fig. 2 (b, c) present the OR images with results of these measurements. As evident, the width of PSF showed a clear depth-dependency following the diameter variation of the laser beam, and the corresponding beam diameter characterized as FWHM along the depth direction is depicted in Fig. 2(c). The highest signal intensity corresponds to the focal distance of the optical illumination (i.e., 0.8 mm from the probe surface), as indicated by the white arrow in Fig. 2 (b). From this specific position, the lateral resolution was estimated to be 13 µm, as illustrated in the inset of Fig. 2 (c). To determine the combined OR and AR resolution, a B-scan image of the phantom was obtained and shown in Fig. 2(d). The detector was kept at 0.5 mm distance from the phantom surface. OR readouts are presented in green while AR measurements are marked in red. As evident, the OR mode can only resolve the first suture (marked by the white arrow) because of optical scattering. The AR mode on the other hand can image much deeper, obtaining a lateral resolution of ~250 µm at depths of at 1.5 mm. Fig. 2 (e) presents the AR resolution as a function of the imaging depth. To demonstrate the volumetric imaging ability of the hybrid endoscope, a four suture phantom was imaged as illustrated in the Fig. 2 (f, insect). The phantom was built by fixing sutures (10 µm in diameter) at two different layers of ~1 mm separation. Afterwards, the sutures were arranged in a luminal

structure, and were scanned cylindrically over 10 degrees. Fig. 2 (f) depicts the corresponding 3D image, showing the overlay of the OR and AR optoacoustic scans.

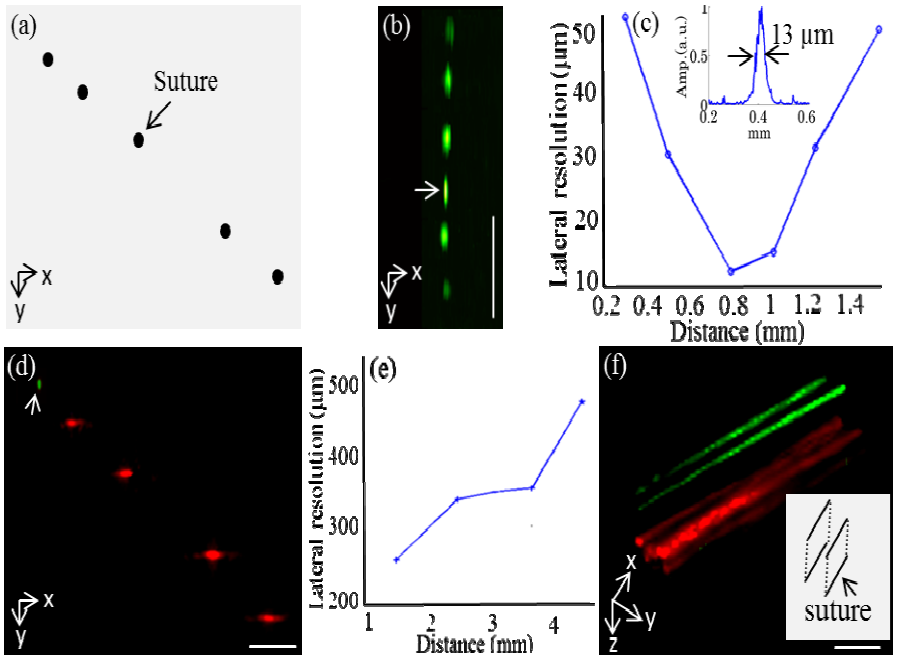


Figure 2. (a) A schematic illustration of the suture phantom. (b) Optoacoustic images of a 10 µm suture imaged with OR illumination at different depths, scale bar 500 µm. (c) Graphical representation of the OR beam diameter characterized as FWHM along with the depth direction. The inset shows a lateral line profile of the suture (indicated by the white arrow in (b)) in the focus region of the GRIN fiber. (d) Optoacoustic images of sutures acquired at different depths with OR and AR illumination, the +y axis corresponds to depth direction, scale bar 1mm. (e) Lateral AR resolution graph along the depth direction. (f) The corresponding 3D image, showing the overlay of normalized OR and AR optoacoustic images of the suture phantom; the +z axis corresponds to depth direction; scale bar 1mm. The OR images are presented in green while the AR image are in red.

For biological tissue experiment, volumetric images were then obtained by scanning the probe cylindrically over 20 degrees and linearly along the lumen longitudinal dimension over 3 mm, with the distance between the mouse ear and the probe kept about 1mm during scanning. By linearly pulling the probe, we acquired sectional images of the mouse ear [indicated by the dash line in Fig. 3(b)] in the AR and OR mode respectively, which are shown in Fig. 3(d) and 3(e). The maximal amplitude projections of the volumetric images acquired in AR and OR modes are shown in Fig. 3(b) and (c) respectively. As can be seen, the AR image resolved the large vessels, which accurately matched those visible in the photograph. Of note, numerous smaller vessels are distinguishable on the OR image, which are not visible on the AR readouts. As an example, the diameter of a specific vessel [marked by the white arrow in (f)] is calculated to be 41 µm as shown in Fig. 3(f). The overlay image in Fig. 3(g) shows the big vessel in AR mode, and small vessels in OR mode.

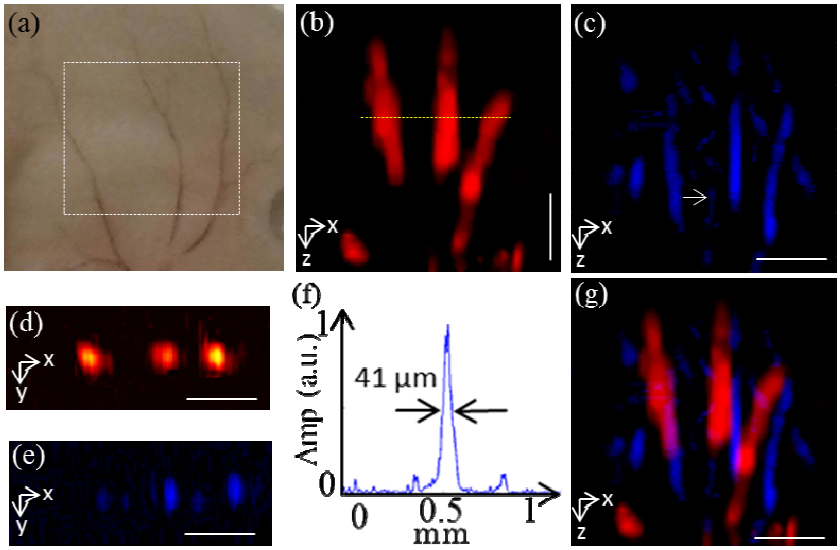


Figure 3. Optoacoustic images of an *ex-vivo* mouse ear. (a) The photograph of the mouse ear shows the scanning area indicated by dash square. (b) and (c) are volumetric maximal amplitude projection images acquired in AR and OR mode respectively, from the mouse ear boxed by the dash square in (a). (d) and (e) are corresponding AR and OR sectional images in the position marked by the yellow dash line in (b). (f) Lateral line profile of the vessel structure indicated by the white arrow in (c). (g) An overlay image, where the red and blue colors represent the AR and OR, respectively. Scale bar 500 µm.

## 4. DISCUSSION AND CONCLUSION

In this letter, we presented the feasibility of hybrid optical resolution and acoustic resolution optoacoustic endoscopy with one sensor. The whole probe has a diameter of 3.6 mm, which can easily pass through the working channel of video endoscopy. By focusing the laser light with the GRIN fiber, we achieved an optical resolution as fine as 13 µm based on the characterization of phantom and tissue samples, and a SNR of 20 dB based on the characterization of a 10 µm diameter suture with the laser energy below the ANSI safety limit (20 mJ/cm2). The results of the suture phantom and ex-vivo mouse ear measurements both show that the hybrid endoscopy system can achieve optical resolution imaging on the surface and tomography imaging for the deeper features. However, it has to be noted, that in the current implementation, due to the short working distance of the OR fiber, the probe has to be close to the sample surface, thus only a small luminal segment can be imaged. To improve the practicability of our setup and to allow imaging the complete lumen, a GRIN fiber with longer focal distance can be applied. Besides, advanced ultrasound transducers, such as optical interferometry based ultrasound detectors, could increase sensitivity and AR resolution [12]. Furthermore, two lasers can be employed in a time-shared fashion to enable parallel acquisition of OR and AR signals in a single scan, which can significantly improve imaging efficiency. Finally, the presented concept of using two different fibers to achieve both OR and AR imaging performance, may impact endoscopic imaging applications by providing additional information not available in previous implementations.

**Funding.** The research leading to these results has received funding from the European Union project FAMOS (FP7 ICT, contract no. 317744).

## REFERENCES


[1] P. Amornphimoltham, A. Masedunskas, and R. Weigert, "Intravital microscopy as a tool to study drug delivery in preclinical studies," Adv Drug Deliv Rev, 63(1-2), 119-28 (2011).

[2] A. Hoffman, M. Goetz, M. Vieth *et al.*, "Confocal laser endomicroscopy: technical status and current indications," Endoscopy, 38(12), 1275-83 (2006).

[3] A. Taruttis, and V. Ntziachristos, "Advances in real-time multispectral optoacoustic imaging and its applications," Nature Photonics, 9(4), 219-227 (2015).

[4] A. Taruttis, G. M. van Dam, and V. Ntziachristos, "Mesoscopic and Macroscopic Optoacoustic Imaging of Cancer," Cancer Res, 75(8), 1548-1559 (2015).

[5] A. Liopo, R. Su, and A. A. Oraevsky, "Melanin nanoparticles as a novel contrast agent for optoacoustic tomography," Photoacoustics, 3(1), 35-43 (2015).

[6] J. M. Yang, C. Favazza, R. Chen *et al.*, "Simultaneous functional photoacoustic and ultrasonic endoscopy of internal organs in vivo," Nat Med, 18(8), 1297-1302 (2012).

[7] H. He, A. Buehler, and V. Ntziachristos, "Optoacoustic endoscopy with curved scanning," Opt Lett, 40(20), 4667-70 (2015).

[8] H. Estrada, J. Turner, M. Kneipp *et al.*, "Real-time optoacoustic brain microscopy with hybrid optical and acoustic resolution," Laser Physics Letters, 11(4), 045601 (2014).

[9] D. Soliman, G. J. Tserevelakis, M. Omar *et al.*, "Combining microscopy with mesoscopy using optical and optoacoustic label-free modes," Sci Rep, 5, 12902 (2015).

[10] E. M. Strohm, M. J. Moore, and M. C. Kolios, "High resolution ultrasound and photoacoustic imaging of single cells," Photoacoustics, (2016).

[11] P. Hajireza, W. Shi, and R. Zemp, "Label-freein vivoGRIN-lens optical resolution photoacoustic micro-endoscopy," Laser Physics Letters, 10(5), 055603 (2013).

[12] A. Rosenthal, S. Kellnberger, D. Bozhko *et al.*, "Sensitive interferometric detection of ultrasound for minimally invasive clinical imaging applications," Laser & Photonics Reviews, 8(3), 450-457 (2014).